Inorg. Chem. **2008**, *47*, 1435−1442

Infrared Spectra and Electronic Structures of Agostic Uranium Methylidene Molecules

Jonathan T. Lyon,[†] Lester Andrews,*[,†] Han-Shi Hu,[‡] and Jun Li*[,‡]

Department of Chemistry, University of Virginia, Charlottesville, Virginia 22904-4319, and Department of Chemistry and Key Laboratory of Organic Optoelectronics and Molecular Engineering of Ministry of Education, Tsinghua University, Beijing 100084, China

Received September 11, 2007

Through reactions of laser-ablated uranium atoms with methylene halides CH_2XY ($XY = F_2$, FCl, and Cl_2), a series of new actinide methylidene molecules $CH_2{=}UF_2$, $CH_2{=}UFCl$, and $CH_2{=}UCl_2$ are formed as the major products. The identification of these complexes has been accomplished via matrix infrared spectra, isotopic substitution, and relativistic density functional calculations of the vibrational frequencies and infrared intensities. Density functional calculations using the generalized gradient approach (PW91) show that these $CH_2{=}UXY$ methylidene complexes prefer highly distorted agostic structures rather than the ethylene-like symmetric structures. The calculated agostic angles (∠H−C−U) are around 89° for all the three uranium complexes, and the predicted vibrational modes and isotopic shifts agree well with experimental values. Electronic structure calculations reveal that these U(IV) molecules all have strong C═U double bonds in the triplet ground states with $5f^2$ configurations. The calculated bond lengths and bond energies indicate that the C═U double bonds are slightly weaker in the fluoride species than in the chloride species because of the radial contraction of the U (6d) orbitals by the inductive effect of the fluorine substituent. The agostic uranium methylidene complexes are compared with analogous transition metal and thorium complexes, which reveal interesting differences in their chemistries.

Introduction

Recent investigations on the reactions of early transition-metal atoms with methane and halomethanes have provided spectroscopic and theoretical evidence for the simple methylidene complexes $CH_2{=}MH_2$ and $CH_2{=}MHX$, which are formed by α-H transfer in the initial energized CH_3-MH and CH_3-MX insertion products.[1−3] Agostic distortion in the methylidene complexes, as measured by the calculated B3LYP and CCSD(T) ∠H−C−M angle and C−H bond length, decreases from Ti to Zr to Hf as the C═M bond length increases, but thorium and uranium reverse this trend with the uranium methylidene complexes exhibiting the largest agostic effect.[1−7] This has recently been documented for a series of $CH_2{=}MH_2$ complexes by using CASSCF/CASPT2 calculations,[8] which confirm the results of earlier B3LYP calculations.[3] However, the higher level ab initio calculations show more agostic distortion than the more approximate density functional method.[9−11]

Our previous research has provided evidence that when group 4 metals react with methylene halides, symmetric $CH_2{=}MX_2$ methylidene complexes are formed rather than

* To whom correspondence should be addressed. E-mail: lsa@virginia.edu (L.A.) and junli@tsinghua.edu.cn (J.L.).
† University of Virginia.
‡ Tsinghua University.

(1) Cho, H.-G.; Andrews, L. *J. Phys. Chem. A* **2004**, *108*, 6294 (Ti + CH_3F).
(2) Cho, H.-G.; Wang, X.; Andrews, L. *J. Am. Chem. Soc.* **2005**, *127*, 465 (Zr + CH_4).
(3) Andrews, L.; Cho, H-G. *Organometallics* **2006**, *25*, 4040 (review article).
(4) Andrews, L.; Cho, H-G. *J. Phys. Chem. A* **2005**, *105*, 6796 (Th + CH_4).
(5) Lyon, J. T.; Andrews, L. *Inorg. Chem.* **2005**, *44*, 8610 (Th + CH_3X).
(6) Lyon, J. T.; Andrews, L.; Malmqvist, P.-Å.; Roos, B. O.; Wang, T.; Bursten, B. E. *Inorg. Chem.* **2007**, *46*, 4917 (U + CH_4).
(7) Lyon, J. T.; Andrews, L. *Inorg. Chem.* **2006**, *45*, 1847 (U + CH_3X).
(8) Roos, B. O.; Lindh, R. H.; Cho, H.-G.; Andrews, L. *J. Phys. Chem. A* **2007**, *111*, 6420 (theoretical study of $CH_2{=}MH_2$.complexes).
(9) Clot, E.; Eisenstein, O. Agostic interactions from a computational perspective. *Structure and Bonding, Computational Inorganic Chemistry*; Kaltzoyannis, N., McGrady, E., Eds.; Springer-Verlag: Heidelberg, Germany, 2004; pp. 1–36.
(10) Scherer, W.; McGrady, G. S. *Angew. Chem., Int. Ed.* **2004**, *43*, 1782.
(11) von Frantzius, G.; Streubel, R.; Brandhorst, K.; Grunenberg, J. *Organometallics* **2006**, *25*, 118.

10.1021/ic701786h CCC: $40.75
Published on Web 02/01/2008

those with agostic distortion.[12–14] A comparison of these results leads to two interesting observations: First, the C═M bond is longer for the difluorides than for the dichlorides, with that of the fluorochloro complexes in between. For example, the theoretically predicted C═Ti bond length in CH_2═TiFCl (1.842 Å) is intermediate between the values of the difluoride (1.850 Å) and the dichloride (1.835 Å). Second, there seems neither agostic distortion for the mixed CH_2═TiFCl methylidene[15] nor for the trifluoro CHF═TiF_2 complex.[13] Furthermore, CH_2═ThF_2 is slightly distorted, whereas CH_2═$ThCl_2$ appears to be more distorted.[16] It will be interesting to determine if the strong agostic effect demonstrated by uranium[6,7] will tip the balance in favor of distortion for the uranium CH_2═UX_2 complexes. The only methylidene complexes to be prepared to date with uranium have come from methane and methyl halide reactions,[6,7] as other efforts in this regard have not found such compounds,[17–21] and the above uranium methylidene dihalide complexes will complement and extend this series. We recently investigated the chiral nature of the CH_2═AnFCl (An = Th, U) complexes, and reported a theoretical analysis in a communication.[22]

Experimental and Theoretical Methods

Laser-ablated U (ORNL, depleted metal) atoms were reacted with the CH_2F_2, CH_2FCl, and CH_2Cl_2 precursors (Du Pont, Fisher) and their isotopic modifications[23] in excess argon (0.5 to 1% concentrations) during condensation onto an 8 K cesium iodide window as described previously.[24] Infrared spectra were recorded on a Nicolet 550 spectrometer after sample deposition, annealing, and irradiation using a 175 W mercury arc street lamp.

The geometry structures and vibrational frequencies of the uranium product complexes were calculated using the hybrid B3LYP density functional method implemented in the Gaussian 98 program[25,26] and generalized gradient approach of PW91 implemented in Amsterdam Density Functional program (ADF 2006.01).[27,28] The B3LYP method was previously employed for the analogous thorium complexes with great success.[4,5,16] In these calculations, we used the SDD pseudopotential and basis set with 32 valence electrons for uranium and the 6-311++G(2d,p) basis set for the light elements.[29] Scalar relativistic effects were included in these calculations through the energy-consistent relativistic pseudopotential.[30] The vibrational frequencies were computed analytically, and zero-point energy (ZPE) corrections were included in the calculation of relative product energies.

To further validate the calculated B3LYP results, the geometries, vibrational frequencies, and electronic structures of the uranium product complexes were also calculated using quasi-relativistic density functional theory (DFT) with the generalized gradient PW91 approach,[28] which has been shown previously to have good performance for actinide complexes.[31] In the PW91 calculations, the zero-order regular approximation (ZORA) was used to account for the scalar and spin–orbit coupling relativistic effects.[32] We used uncontracted Slater basis sets with quality of triple-ζ plus two polarization functions (TZ2P).[33] The frozen core approximation was applied to the [$1s^2$] cores of C and F, [$1s^2-2p^6$] core of Cl, and [$1s^2-5d^{10}$] core of U, with the rest of the electrons explicitly treated variationally.[34] The geometries were fully optimized with inclusion of the scalar relativistic effects. Vibrational frequency calculations were accomplished by numerical differentiation of the energy gradients.

Results and Discussion

Reactions of laser-ablated U atoms with difluoro-, fluorochloro-, and dichloromethane precursors in excess argon during condensation will be presented. These experiments also produced transient free radicals and molecular ions that are formed by the precursor photochemistry, which are common to similar reactions involving other metal atoms and have been identified previously.[22,35–37] In addition, weak

(12) Lyon, J. T.; Andrews, L. *Organometallics* **2006**, *25*, 1341.
(13) Lyon, J. T.; Andrews, L. *Inorg. Chem.* **2007**, *46*, 4799 (Gr 4 + CH_2F_2).
(14) Lyon, J. T.; Andrews, L. *Organometallics* **2007**, *26*, 332 (Gr 4 + CH_2Cl_2).
(15) Lyon, J. T.; Andrews, L. Unpublished calculation for CH_2═TiFCl, 2007.
(16) Lyon, J. T.; Andrews, L. *Eur. J. Inorg. Chem.* **2008**, ASAP (Th + CH_2X_2, CHX_3, CX_4).
(17) Cremer, R. E.; Maynard, R. B.; Paw, J. C.; Gilje, J. W. *J. Am. Chem. Soc.* **1981**, *103*, 3589.
(18) Pool, J. A.; Scott, B. L.; Kiplinger, J. L. *J. Am. Chem. Soc.* **2005**, *127*, 1338.
(19) Burns, C. J. *Science* **2005**, *309*, 1823.
(20) Schrock, R. R. *Chem. Rev* **2002**, *102*, 145.
(21) (a) Herndon, J. W. *Coord. Chem. Rev.* **2005**, *249*, 999. (b) Herndon, J. W. *Coord. Chem. Rev.* **2006**, *250*, 1889.
(22) Li, J.; Hu, H.-S.; Lyon, J. T.; Andrews, L. *Angew. Chem., Int. Ed.* **2007**, *46*, 9045; *Angew. Chem.* **2007**, *119*, 9203 (CH_2═AnFCl).
(23) (a) Andrews, L.; Prochaska, F. T. *J. Chem. Phys.* **1979**, *70*, 4714 and references therein. (b) Andrews, L.; Willner, H.; Prochaska, F. T. *J. Fluorine Chem.* **1979**, *13*, 273.
(24) (a) Souter, P. F.; Kushto, G. P.; Andrews, L.; Neurock, M. *J. Am. Chem. Soc.* **1997**, *119*, 1682 (U + H_2). (b) Andrews, L.; Citra, A. *Chem. Rev* **2002**, *102*, 885 and references therein.
(25) (a) Becke, A. D. *J. Chem. Phys.* **1993**, *98*, 5648. (b) Lee, C.; Yang, W.; Parr, R. G. *Phys. Rev. B* **1988**, *37*, 785.
(26) Frisch, M. J.; Trucks, G. W.; Schlegel, H. B.; Scuseria, G. E.; Robb, M. A.; Cheeseman, J. R.; Zakrzewski, V. G.; Montgomery, J. A., Jr.; Stratmann, R. E.; Burant, J. C.; Dapprich, S.; Millam, J. M.; Daniels, A. D.; Kudin, K. N.; Strain, M. C.; Farkas, O.; Tomasi, J.; Barone, V.; Cossi, M.; Cammi, R.; Mennucci, B.; Pomelli, C.; Adamo, C.; Clifford, S.; Ochterski, J.; Petersson, G. A.; Ayala, P. Y.; Cui, Q.; Morokuma, K.; Rega, N.; Salvador, P.; Dannenberg, J. J.; Malick, D. K.; Rabuck, A. D.; Raghavachari, K.; Foresman, J. B.; Cioslowski, J.; Ortiz, J. V.; Baboul, A. G.; Stefanov, B. B.; Liu, G.; Liashenko, A.; Piskorz, P.; Komaromi, I.; Gomperts, R.; Martin, R. L.; Fox, D. J.; Keith, T.; Al-Laham, M. A.; Peng, C. Y.; Nanayakkara, A.; Challacombe, M.; Gill, P. M. W.; Johnson, B.; Chen, W.; Wong, M. W.; Andres, J. L.; Gonzalez, C.; Head-Gordon, M.; Replogle, E. S.; Pople, J. A. *Gaussian 98*, revision A.11.4; Gaussian, Inc.: Pittsburgh, PA, 2002.
(27) (a) *ADF*, 2006.01; SCM, Theoretical Chemistry, Vrije Universiteit: Amsterdam, The Netherlands, 2006 (http://www.scm.com); te Velde, G.; Bickelhaupt, F. M.; van Gisbergen, S. J. A.; Fonseca Guerra, C.; Baerends, E. J.; Snijders, J. G.; Ziegler, T. *J. Comput. Chem.* **2001**, *22*, 931. (b) Fonseca Guerra, C.; Snijders, J. G.; te Velde, G.; Baerends, E. J. *Theor. Chem. Acc.* **1998**, *99*, 391.
(28) Perdew, J. P.; Wang, Y. *Phys. Rev. B* **1992**, *45*, 13244.
(29) (a) Frisch, M. J.; Pople, J. A.; Binkley, J. S . *J. Chem. Phys.* **1984**, *80*, 3265. (b) McLean, A. D.; Chandler, G. S. *J. Chem. Phys.* **1980**, *72*, 5639.
(30) Küchle, W.; Dolg, M.; Stoll, H.; Preuss, H. *J. Chem. Phys.* **1994**, *100*, 7535.
(31) (a) Li, J.; Bursten, B. E. *J. Am. Chem. Soc.* **1998**, *120*, 11456. (b) Li J.; Bursten, B. E. In *Computational Organometallic Chemistry*; Cundari, T. R., Ed.; Marcel Dekker: New York, 2001; pp. 345–379.
(32) van Lenthe, E.; Baerends, E. J.; Snijders, J. G. *J. Chem. Phys.* **1993**, *99*, 4597.
(33) van Lenthe, E.; Baerends, E. J. *J. Comput. Chem.* **2003**, *24*, 1142.
(34) Baerends, E. J.; Ellis, D. E.; Ros, P. *Chem. Phys.* **1973**, *2*, 42.
(35) Carver, T. G.; Andrews, L. *J. Chem. Phys.* **1969**, *50*, 5100.
(36) Prochaska, F. T.; Keelan, B. W.; Andrews, L. *J. Mol. Spectrosc.* **1979**, *76*, 142.
(37) Kelsall, B. J.; Andrews, L. *J. Mol. Spectrosc.* **1983**, *97*, 362.

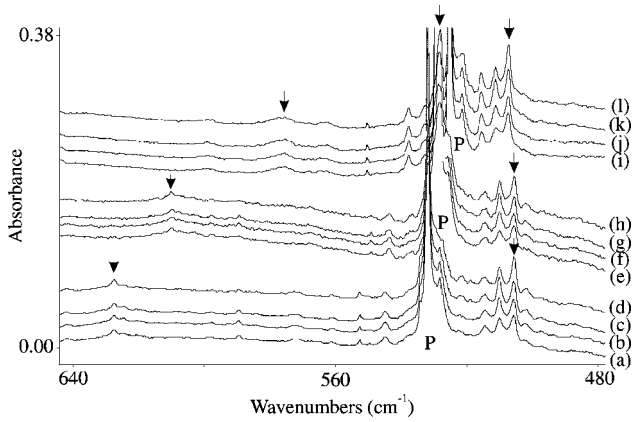

Figure 1. Infrared spectra in the 640–480 cm^{-1} region for laser ablated U atoms codeposited with CH_2F_2 in excess argon at 8 K. (a) U and 0.2% CH_2F_2 in argon codeposited for 1 h, (b) after >290 nm irradiation, (c) after >220 nm irradiation, and (d) after annealing to 30 K. (e) U and 0.2% $^{13}CH_2F_2$ in argon codeposited for 1 h, (f) after >290 nm irradiation, (g) after >220 nm irradiation, and (h) after annealing to 30 K. (i) U and 0.2% CD_2F_2 in argon codeposited for 1 h, (j) after >290 nm irradiation, (k) after >220 nm irradiation, and (l) after annealing to 30 K. P denotes methylene fluoride precursor absorptions. Arrows indicate major product bands.

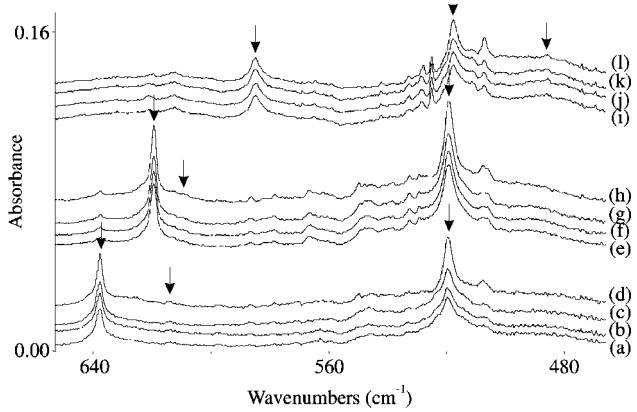

Figure 2. Infrared spectra in the 640–480 cm^{-1} region for laser ablated U atoms codeposited with CH_2FCl in excess argon at 8 K. (a) U and 0.8% CH_2FCl in argon codeposited for 1 h, (b) after >290 nm irradiation, (c) after >220 nm irradiation, and (d) after annealing to 30 K. (e) U and 0.7% $^{13}CH_2FCl$ in argon codeposited for 1 h, (f) after >290 nm irradiation, (g) after >220 nm irradiation, and (h) after annealing to 30 K. (i) U and 0.6% CD_2FCl in argon codeposited for 1 h, (j) after >290 nm irradiation, (k) after >220 nm irradiation, and (l) after annealing to 30 K. Arrows indicate major product bands.

bands were also observed for uranium oxides.[38] We will present the results of the major reaction product molecules in the following sections. Figures 1, 2, and 3 show the experimental infrared spectra of products of U reacting with CH_2F_2, CH_2FCl, and CH_2Cl_2. Figure 4 illustrates the optimized structures of the three product complexes from scalar relativistic ZORA and PW91/TZ2P calculations. The orbital interactions between the CH_2 and UF_2 fragments to form the symmetric and distorted agostic $CH_2{=}UF_2$ structures are shown in Figure 5, and the isosurfaces of the Kohn–Sham molecular orbitals of the two singly occupied U 5f orbitals and the C=U double bonds are shown in Figure 6. In addition, Tables 1, 2, and 3 list the observed and calculated B3LYP and PW91 fundamental vibrational frequencies and infrared intensities of the major reaction products. The experimental matrix infrared spectra are assigned on the basis of their agreement with the calculated harmonic vibrational modes. It should be pointed out that the matrix effects and anharmonic corrections were not included in the computational research. Preliminary calculations on $CH_2{=}UF_2$ show that the anharmonic effects reduce the antisymetric U−F stretching frequency by some 11 cm^{-1}, bringing it closer to the matrix experimental value. The optimized geometry parameters and calculated diabatic C=U bond energies without spin–orbit coupling effects are listed in Table 4 to reveal the structure and energetic difference among the products with different halogen substituents. The calculated natural charges and Wiberg bond orders are listed in Table 5, and the natural localized molecular orbitals and the natural hybrid orbitals of the covalent bonds of three major products are listed in Table 6.[39,40]

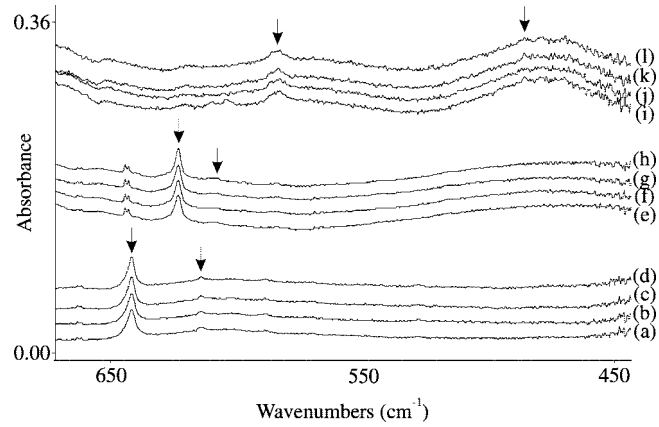

Figure 3. Infrared spectra in the 670–450 cm^{-1} region for laser ablated U atoms co-deposited with CH_2Cl_2 in excess argon at 8 K. (a) U and 1% CH_2Cl_2 in argon co-deposited for 1 h, (b) after >290 nm irradiation, (c) after >220 nm irradiation, and (d) after annealing to 30 K. (e) U and 1% $^{13}CH_2Cl_2$ in an argon co-deposited for 1 h, (f) after >290 nm irradiation, (g) after >220 nm irradiation, and (h) after annealing to 30 K. (i) U and 1% CD_2Cl_2 in argon co-deposited for 1 h, (j) after >290 nm irradiation, (k) after >220 nm irradiation, and (l) after annealing to 30 K. Arrows indicate major product bands.

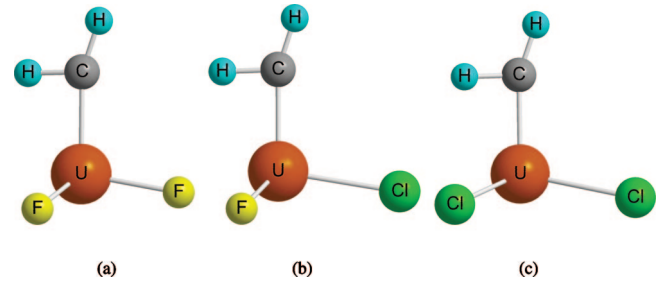

Figure 4. Structures theoretically optimized for the uranium methylidene complexes $CH_2{=}UF_2$ (a), $CH_2{=}UFCl$ (b), and $CH_2{=}UCl_2$ (c) using the scalar relativistic ZORA and PW91/TZ2P method. The calculated bond lengths and angles are listed in Table 4 (atom colors: U, orange; C, gray; F, yellow; Cl, green).

CH_2F_2. The reaction of laser-ablated U atoms with CH_2F_2 gives major new infrared absorptions labeled with arrows at

(38) Hunt, R. D.; Andrews, L. *J. Chem. Phys.* **1993**, *98*, 3690 and references therein.

(39) (a) Reed, A. E.; Weinstock, R. B.; Weinhold, F. *J. Chem. Phys.* **1985**, *83*, 735. (b) Reed, A. E.; Curtiss, L. A.; Weinhold, F. *Chem. Rev.* **1988**, *88*, 899.

(40) Wiberg, K. B. *Tetrahedron* **1968**, *24*, 1083.

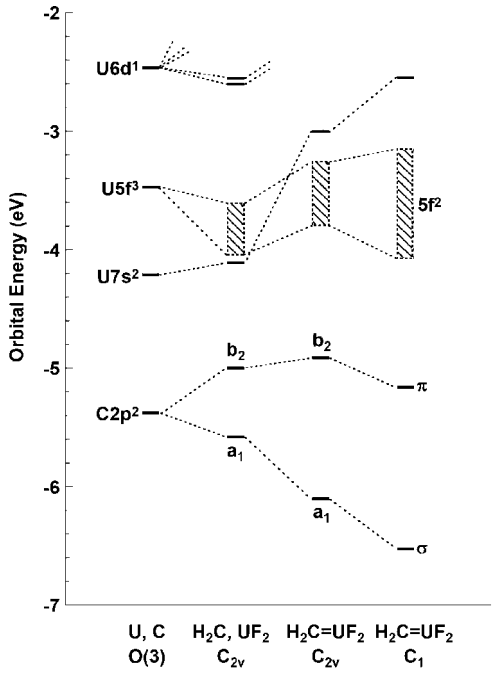

Figure 5. Energy levels of the U and C atomic orbitals, CH_2 and UF_2 fragment molecular orbitals, and the orbitals of the symmetric (C_{2v}) and agostic (C_1) $H_2C{=}UF_2$ molecule. The $5f^2$-manifold of U orbitals is shown as a shaded block. In the agostic structure, the pseudo-σ and -π orbitals represent the C=U double bond. All the energies are from ZORA PW91 calculations.

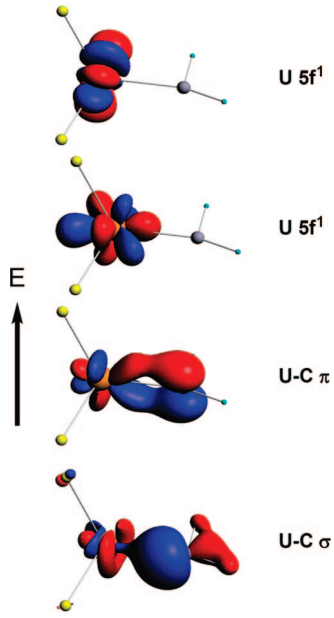

Figure 6. Isosurfaces of the Kohn–Sham molecular orbitals of the singly occupied U 5f orbitals and the pseudo σ- and π-type orbitals of the C=U bonds in $CH_2{=}UF_2$ (isosurface value=0.1 au).

627.6 cm^{-1} and as a matrix split trio at 514.7, 509.9, and 505.5 cm^{-1}. These bands increase slightly with two UV irradiations and sharpen on annealing to 30 K, as shown in Figure 1. Also included in Figure 1 are spectra for the reaction of U with $^{13}CH_2F_2$ and CD_2F_2. Carbon-13 isotopic substitution shifted the weaker band to 610.0 cm^{-1} but did not shift the trio of bands. Deuterium substitution shifted the upper band to 575.4 cm^{-1} and blue-shifted the trio to 515.6, 511.2, and 507.4 cm^{-1}. In addition the strong precursor band (labeled P) red-shifted such that another product absorption was now observed at 528.3 cm^{-1}, which was covered by the strong precursor band for the hydrogen isotopic precursors. Finally, the weak band at 544.8 cm^{-1} (not labeled) increases slightly on >290 nm irradiation, decreases slightly with >220 nm light, and shifts to 543.6 cm^{-1} with carbon-13 and to 537.6 cm^{-1} with deuterium isotopic substitution.

Our previous research indicates that the reaction of U with CH_3F goes through the $CH_3{-}UF$ intermediate, followed by α-H transfer to give the methylidene, $CH_2{=}UHF$. Both products were observed in the previous matrix sample although upon ultraviolet irradiation the $CH_3{-}UF$ intermediate is favored, which is calculated to be 21 kcal/mol lower in energy by using B3LYP approach.[7] Here, without accounting for spin–orbit coupling effects, the methylidene $CH_2{=}UF_2$ complex is calculated to be 49 kcal/mol lower in energy than the first insertion product $CH_2F{-}UF$, where the thermodynamic driving force of the strong U−F bond plays a vital role. Again ultraviolet irradiation is required to activate the reaction by excitation of atomic uranium. The choice of α-H transfer versus α-F transfer in the energized insertion product first formed is governed by thermochemistry because $CH_2{=}UF_2$ methylidene is much lower in energy than CHF=UHF, on the basis of our calculations. In like fashion, the $HC{\equiv}UHF_2$ methylidyne product was not observed because it is 49 kcal/mol higher in energy than the $CH_2{=}UF_2$ methylidene complex. Therefore, the experimental results indicate that the reactions between U atom and CH_2F_2 likely proceed in the following mechanism:

$$U^* + CH_2F_2 \rightarrow CH_2F{-}UF^* \rightarrow CH_2{=}UF_2 \qquad (1)$$

Although the analogous group 4 complexes[12–14] were computed to be symmetrical, uranium prefers more agostic distortion than the transition metals.[8] Our DFT calculation of $CH_2{=}UF_2$ predicted a distorted structure with the B3LYP functional $\angle H_{ag}{-}C{-}U$ angle of 101.6°, which is significantly larger than the 88.9° angle calculated using PW91 (Table 4). The pure density functional is probably more accurate than the hybrid one here because the former also gives larger agostic angles than benchmark CASPT2 calculations.[8] Hereafter, we denote the agostic and nonagostic hydrogen atoms as H_{ag} and H_{ax} because the nonagostic hydrogen atoms are located in the axial directions with regard to the C=U bond axis. The calculated isotopic shifts define the vibrational modes. The calculated B3LYP spin expectation value, $<s^2> = 2.15$, is significantly higher than that of a pure triplet state (2.00), indicating spin contamination resulting from quintet or other high-spin states. The two strongest infrared absorptions are predicted at 544 and 528 cm^{-1} at the B3LYP level, and these are the diagnostic U−F stretching modes as UF_4 (doublet 537.4, 532.5 cm^{-1} in solid argon) absorbs in this region.[41–44] The trio headed by 505.5 cm^{-1} is assigned to the stronger antisymmetric U−F stretching mode, and the

(41) Kunze, K. R.; Hauge, R. H.; Hammill, D.; Margrave, J. L. *J. Phys. Chem.* **1977**, *81*, 1644.
(42) Hunt, R. D.; Thompson, C.; Hassanzadeh, P.; Andrews, L. *Inorg. Chem.* **1994**, *33*, 388 and references therein.
(43) Souter, P. F.; Andrews, L. *J. Mol. Struct.* **1997**, *412*, 161.

Table 1. Observed and Calculated Fundamental Frequencies of $CH_2{=}UF_2$ in the Triplet Ground Electronic State[a,b]

	$CH_2{=}UF_2$			$^{13}CH_2{=}UF_2$			$CD_2{=}UF_2$		
mode description[c]	obsd	B3LYP	PW91	obsd	B3LYP	PW91	obsd	B3LYP	PW91
CH stretch		3130(7)	3072(1)		3120(8)	3062(1)		2310(2)	2266(2)
CH stretch		2885(45)	2675(43)		2879(46)	2669(44)		2101(18)	1946(17)
CH_2 bend		1331(16)	1315(46)		1324(15)	1309(47)		1010(10)	993(24)
C=U stretch	627.6		651(83)	610.0		632(77)	575.4		596(72)
CH_2 wag	very weak	624(138)	614(116)	weak	616(135)	609(114)	weak	508(49)	447(57)
U−F stretch, sym		544(153)	562(128)		544(151)	561(127)	528.3	544(132)	560(127)
U−F stretch, antisym	505.5	528(166)	539(131)	505.5	527(169)	539(131)	507.4	530(216)	539(159)
C=U stretch, CH_2 def		511(19)	517(4)		500(15)	513(4)		445(38)	394(3)
CH_2 def		305(2)			302(2)			236(1)	
CH_2 rock		202(5)	208(1)		201(5)	208(1)		169(7)	153(1)
C−U−F_2 dist		143(3)	128(2)		142(3)	128(2)		129(5)	122(2)
F−U−F bend		131(16)	109(7)		130(16)	108(7)		126(9)	104(7)
deformation		99(12)	106(7)		98(12)	105(7)		89(12)	100(4)

[a] Observed frequencies in argon matrix. [b] Calculated B3LYP/6-311++G(2d,p)/SDD and PW91/TZ2P frequencies and infrared intensities (in parenthesis) are in cm^{-1} and km/mol. [c] The predominantly C=U stretching mode falls in a different position with each calculation so this mode is listed twice in the description, but only one numerical value is given so that there are twelve total calculated frequencies for each isotopic molecule.

precursor covers the symmetric counterpart, but both are observed for $CD_2{=}UF_2$ at 528.3 and 507.4 cm^{-1}.

The weaker upper band at 627.6 cm^{-1} is near the CH_2 wagging motion calculated at 624 cm^{-1} and defined by the isotopic shifts, but the observed isotopic shifts do not seem to fit those calculated for the B3LYP vibrational assignment. For example, the calculated carbon-13 shift for the wagging mode, 7.4 cm^{-1}, is far smaller than the observed shift of 17.6 cm^{-1}. Furthermore, for the analogous $CH_2{=}UHF$ complex the B3LYP calculated and observed C=U stretching mode were 618 and 659.4 cm^{-1}, which have carbon-13 shifts of 15 and 19 cm^{-1}, respectively, and the spin contamination was less ($<s^2> = 2.08$).[7] This comparison shows clearly that the B3LYP hybrid density functional calculation does not predict the C=U stretching mode observed for $CH_2{=}UF_2$ at 627.6 cm^{-1} in the correct region because the B3LYP calculated C=U stretching mode (511 cm^{-1}) is much lower.

In contrast, the PW91 calculations reveal more agostic distortion, as shown in Figure 4. The PW91 vibrational frequencies predict the C=U stretching mode at 651 cm^{-1}, which lies in the correct region of absorption. The calculated and observed carbon-13 shifts, 19.0 and 17.6 cm^{-1}, and deuterium shifts, 55.8 and 52.2 cm^{-1}, respectively, are in good agreement for this carbon−uranium double-bonded uranium molecule. On the other hand, both B3LYP and PW91 calculations predict significant infrared intensities for the CH_2 wagging mode, while this band is not observed in the aforementioned matrix experiment, and an additional experiment using 1% CH_2F_2 concentration still failed to increase the product yield. This subtle discrepancy could be caused by either the harmonic approximation used in the DFT calculations or the effective quenching of this mode in the solid matrix environment. The assumed CD_2 wagging mode below 500 cm^{-1} is manifest in the blue deuterium shift for the U−F stretching mode (calculated 0.2 cm^{-1}, observed 1.9 cm^{-1}) because of the relaxation of this vibrational interaction. However, with increased product yields for the following analogous methylidene complexes, the CH_2 wagging mode is indeed detected at the predicted frequency, despite being much weaker than predicted by calculations.

CH_2FCl. Reaction of U with CH_2FCl produced the three new absorptions, illustrated in Figure 2, at 637.8, 614.6, and 519.7 cm^{-1}. These absorptions are increased by 10% upon >220 nm irradiation. The carbon-13 substituted precursor provided absorptions at 619.5, 609.5, and 519.5 cm^{-1}, and CD_2FCl reaction yielded bands at 585.2, 517.9, and 485.5 cm^{-1}.[22]

The B3LYP calculation revealed agostic distortion ($\angle H_{ag}$−C−U angle 96.6°), but the $<s^2>$ value of 2.13 also shows spin contamination. The predicted C=U stretching mode at 547 cm^{-1} is again too low, indicating that the B3LYP calculation simply does not produce the correct vibrational mode mixing. The PW91 frequencies listed in Table 2 reveal excellent agreement between the calculated and the observed isotopic shifts for the three vibrational modes of the C=U stretch, the CH_2 wag, and the U−F stretch. For carbon-13, the calculated C=U stretching mode at 654 cm^{-1} is just above the observed value 637.8 cm^{-1}, and the calculated frequency shift (19.2 cm^{-1}) matches well with the observed shift (18.3 cm^{-1}). Likewise, the calculated CH_2 wagging mode at 619 cm^{-1} with 5.4 cm^{-1} shift fits the weak 614.6 cm^{-1} band with 5.1 cm^{-1} shift, and the U−F mode predicted at 560 cm^{-1} is appropriate for the 519.7 cm^{-1} absorption; both have 0.2 cm^{-1} shifts. For deuterium, the calculated C−U stretching mode exhibits a 56.9 cm^{-1} shift, and the observed band is shifted 52.6 cm^{-1}; the U−F mode is calculated to shift 1.0 cm^{-1}, and the observed bands define a 1.8 cm^{-1} shift. The agreement between the calculated harmonic and experimental matrix frequency is again worse for the CH_2 wagging mode, which has a calculated harmonic shift of 136.5 cm^{-1} and an observed shift of 129.1 cm^{-1}. This $CH_2{=}UFCl$ molecule represents an interesting example of chriality in f-element complexes, as discussed elsewhere.[22]

CH_2Cl_2. Reaction of U and CH_2Cl_2 produced strong absorption at 642.1 cm^{-1} and weak absorption at 614.5 cm^{-1}, which are increased 10% on full arc irradiation, as shown in Figure 3. These absorptions are shifted to 623.6 and 608.5 cm^{-1} and to 583.7 and 486.0 cm^{-1}, respectively, with the $^{13}CH_2Cl_2$ and CD_2Cl_2 reagents. These results reveal that

(44) Konings, R. J. M.; Hildenbrand, D. L. *J. Alloys Compd.* **1998**, *583*, 271–273.

Table 2. Observed and Calculated Fundamental Frequencies of CH_2═UFCl in the Triplet Ground Electronic State[a,b]

	CH_2═UFCl			$^{13}CH_2$═UFCl			CD_2═UFCl		
mode description	obsd	B3LYP	PW91	obsd	B3LYP	PW91	obsd	B3LYP	PW91
CH stretch		3138(3)	3072(1)		3128(4)	3062(1)		2315(1)	2267(2)
CH stretch		2847(32)	2701(18)		2824(33)	2695(19)		2069(11)	1965(6)
CH_2 bend		1339(22)	1317(33)		1331(22)	1310(33)		1016(16)	994(23)
C═U stretch	637.8		654(92)	619.5		635(88)	585.2		597(77)
CH_2 wag	614.6	627(132)	619(97)	609.5	620(130)	614(93)	485.5	471(57)	482(71)
C═U stretch		547(28)			533(27)			516(28)	
U−F stretch	519.7	537(149)	560(144)	519.5	538(146)	560(144)	517.9	538(186)	559(138)
CH_2 def		346(12)	505(3)		343(15)	501(3)		262(1)	384(4)
U−Cl stretch		306(70)	316(60)		306(69)	316(60)		309(80)	316(58)
CH_2 def		210(3)	178(1)		209(3)	178(1)		153(2)	132(1)
CH_2 rock		113(6)	122(3)		111(5)	120(3)		105(6)	113(2)
C−U−F or Cl dist		103(10)	96(1)		102(10)	94(1)		98(9)	90(1)
F−U−Cl bend		83(2)	68(6)		82(2)	68(6)		79(2)	64(5)

[a] Observed frequencies in argon matrix. [b] Calculated B3LYP/6-311++G(2d,p)/SDD and PW91/TZ2P frequencies and infrared intensities (in parenthesis) are in cm^{-1} and km/mol. Mode descriptions differ slightly for the two different density functional methods.

Table 3. Observed and Calculated Fundamental Frequencies of CH_2═UCl_2 in the Triplet Ground Electronic State[a,b]

	CH_2═UCl_2			$^{13}CH_2$═UCl_2			CD_2═UCl_2		
mode description	obsd	B3LYP	PW91	obsd	B3LYP	PW91	obsd	B3LYP	PW91
CH stretch		3098(6)	3075(1)		3087(6)	3065(0)		2295(1)	2270(3)
CH stretch		3018(11)	2692(13)		3013(11)	2686(13)		2187(7)	1960(4)
CH_2 bend		1316(7)	1320(28)		1309(7)	1314(28)		997(3)	997(24)
C═U stretch	642.1	345(3)	660(91)	623.6	337(5)	641(88)	583.7	313(43)	602(70)
CH_2 wag	614.5	573(146)	618(95)	608.5	567(142)	612(90)	486.0	454(104)	482(70)
CH_2 def			510(6)			507(6)			388(9)
U−Cl stretch, sym		315(117)	325(61)		315(114)	325(61)		316(80)	325(55)
U−Cl stretch, antisym		303(49)	319(58)		301(48))	319(59)		296(43)	318(58)
CH_2 def		232(4)	166(1)		230(4)	166(1)		175(1)	122(1)
CH_2 rock		136(6)	112(1)		133(6)	110(1)		124(5)	101(1)
C−U−Cl_2 dist		72(2)	80(1)		71(2)	78(1)		69(3)	75(1)
Cl−U−Cl bend		55(8)	59(4)		54(8)	59(4)		50(10)	58(4)
deformation		40(5)			40 (5)			31(1)	

[a] Observed frequencies in argon matrix. [b] Calculated B3LYP/6-311++G(2d,p)/SDD and PW91/TZ2P frequencies and infrared intensities (in parenthesis) are in cm^{-1} and km/mol. The B3LYP calculations erroneously predict a symmetric structure, whereas the PW91 calculations locate an agostic structure. Mode descriptions differ slightly for the two different density functional methods.

CH_2═UCl_2 has been formed as the major product. Notice that the first absorption in each figure is stronger in the order CH_2Cl_2 > CH_2FCl >> CH_2F_2, indicating that carbon−chlorine bond activation is more favorable than carbon−fluorine bond activation because the latter is a much stronger bond.

As we observed earlier, the agostic angle predicted by the B3LYP functional is larger than those from PW91 calculations. In fact, the agostic angle computed using B3LYP is so large for CH_2═UCl_2 that only a symmetric structure is located. The B3LYP functional predicted an ethylene-like symmetric structure for CH_2═UCl_2, and the expectation value, $<s^2>$ (2.26), shows substantial spin contamination. The C═U stretching mode is calculated as 345 cm^{-1}, which is simply incorrect. The PW91 calculations shows that the molecule is indeed distorted with an agostic angle of $\angle H_{ag}-C-U = 88.5°$. The C═U stretching mode is predicted at 660 cm^{-1} with a 58 cm^{-1} deuterium shift, which is once again in good agreement with the observed 642.1 cm^{-1} band and the 58.4 cm^{-1} shift (Table 3), particularly when considering that matrix effects tend to reduce the stretching frequencies. In addition the CH_2 wagging mode was predicted at 618 cm^{-1} with a 136 cm^{-1} deuterium shift, and the observed band is at 614.5 cm^{-1} with deuterium shift of 128.5 cm^{-1}. Hence, the PW91 functional performs well in the description of the strong skeletal vibrational modes of CH_2═UCl_2, as we have come to expect of density functional methods for describing more typical molecules.[45,46] Notice better agreement for the C═U stretching mode than for the CH_2 wagging mode because the latter is expected to be more anharmonic.

Table 4. Optimized Geometry Parameters and Diabatic C═U Bond Energies of CH_2═UX_2 Complexes Calculated Using ZORA PW91 Approach[a]

	CH_2═UF_2	CH_2═UFCl	CH_2═UCl_2
U···H_{ag}	2.339	2.336	2.316
C−H_{ag}	1.135	1.133	1.134
C−H_{ax}	1.094	1.094	1.094
U−X_{in}	2.050	2.528	2.523
U−X_{out}	2.062	2.048	2.501
C═U	2.066	2.058	2.049
$\angle H_{ag}CU$	88.9	89.2	88.5
HCH	110.7	110.4	110.5
$\angle X_{in}UX_{out}$	99.6	105.0	106.3
$\angle X_{in}UCH_{ag}$	5.3	13.6	22.8
BE	109	110	113

[a] All the bond distances are in Å; bond angles are in degrees, and bond energies in kcal/mol. H_{ax} and H_{ag} are the hydrogen atoms lying on the axial and equatorial directions with regard to the C═U axis. The X_{in} and X_{out} are the halogen ligands lying inside and outside the H_2C═U plane.

Finally, it is of interest to compare the common frequencies observed for the CH_2═UHX and CH_2═UX_2 methylidene complexes.[7] The C═U stretching modes are higher for the

(45) Scott, A. P.; Radom, L. *J. Phys. Chem.* **1996**, *100*, 16502.
(46) von Frantzius, G.; Streubel, R.; Brandhorst, K.; Grunenberg, J. *Organometallics* **2006**, *25*, 118.

Table 5. Calculated Wiberg Bond Orders (BO) and Natural Charges (q) from NBO Analysis

bond	BO	q_N
	CH_2═UF_2	
U═C	1.44	U (2.52), C (−1.34)
U···H_{ag}	0.04	U (2.52), H (0.13)
C−H_{ag}	0.94	C (−1.34), H (0.13)
C−H_{ax}	0.93	C (−1.34), H (0.20)
U−F_{in}	0.45	U (2.52), F (−0.76)
U−F_{out}	0.48	U (2.52), F (−0.75)
	CH_2═UFCl	
U═C	1.46	U (2.42), C (−1.33)
U···H_{ag}	0.05	U (2.42), H (0.14)
C−H_{ag}	0.92	C (−1.33), H (0.14)
C−H_{ax}	0.93	C (−1.33), H (0.20)
U−F_{in}	0.45	U (2.42), F (−0.75)
U−Cl_{out}	0.58	U (2.42), Cl (−0.68)
	CH_2═UCl_2	
U═C	1.48	U (2.30), C (−1.32)
U···H_{ag}	0.05	U (2.30), H (0.15)
C−H_{ag}	0.92	C (−1.32), H (0.15)
C−H_{ax}	0.93	C (−1.32), H (0.20)
U−Cl_{in}	0.59	U (2.30), Cl (−0.67)
U−Cl_{out}	0.61	U (2.30), Cl (−0.66)

monofluoride and -chloride complexes by 32 and 29 cm^{-1}, respectively, and the additional halide substituents appear to contract the U 6d/5f orbitals and to make them less effective in π-bonding to carbon. The CH_2 wagging mode is 611.6 cm^{-1} for the monofluoride complex, but it is too weak to be observed for the difluoride complex; however, these modes are observed at 600.5 and 614.5 cm^{-1}, respectively, for the monochloride and dichloride complexes. The U−F stretching mode for the monofluoride complex at 522.5 cm^{-1} is just above the observed 505.5 cm^{-1} antisymmetric mode for the difluoride complex.

Structure and Bonding. We have shown so far that when comparing with experiments, the PW91 functional of the generalized gradient approach best describes the structures, vibrational frequencies, and isotopic frequency shifts of the uranium methylidene complexes, consistent with our previous observation.[31] As illustrated in Figure 4 and Table 4, the CH_2═UXY structures all show considerable agostic distortion with agostic ∠H_{ag}−C−U angles of 88.9°, 89.2°, and 88.5° for CH_2═UF_2, CH_2═UFCl, and CH_2═UCl_2, respectively. These agostic structures are in direct contrast with those of analogous transition-metal complexes such as CH_2═WF_2, where a nonagostic C_{2v}-symmetric structure with C═W distance of 1.89 Å and H−C−W angle 122.8° are computed. In addition, the C−H_{ax} and C−H_{ag} bonds were calculated as 1.094 and 1.133 ± 0.001 Å, respectively, in CH_2═UXY, which indicates considerable C−H bond elongation caused by the agostic distortion. As shown by the dihedral angles ∠$X_{in}UCH_{ag}$ listed in Table 4, an interesting feature of these agostic structures is that one of the U−X bonds is almost always coplanar with the plane of U═C−H_{ag}, likely because of dipole interactions (Figure 4). The halogen atoms are accordingly labeled as in-plane (X_{in}) and out-of-plane (X_{out}). For CH_2═UXY, the energy difference of the isomers with X_{in} and X_{out} is rather small. For instance, the two CH_2═UFCl isomers with F_{in} and F_{out} differ in energy by 2.1 kcal/mol (PW91) or 0.7 kcal/mol (B3LYP), and the energy difference lies within the error bar of the DFT methods used. The ∠$X_{in}UCH_{ag}$ dihedral angle increases from CH_2═UF_2 to CH_2═UFCl to CH_2═UCl_2, consistent with the reduced dipole moment of the U−halogen bonds from F to Cl.

As exemplified by the energy-level diagrams of the calculated molecular orbitals of CH_2═UF_2, electronic structures of these uranium methylidene molecules can be interpreted by the orbital interactions between U and C and between the UXY and CH_2 fragments. As shown in Figure 5, in addition to the σ-bond framework the C 2p orbitals form the $a_1 + b_2$ representations in CH_2, which are further split through orbital interaction with orbitals of UF_2, when forming a C_{2v}-symmetric CH_2═UF_2 molecule. The two $a_1 + b_2$ molecular orbitals are the basis of the C═U double bonds, which have approximately σ- and π-type bonding between C and U, as shown by the isosurfaces of the calculated Kohn–Sham orbitals (Figure 6). They are further stabilized through agostic interaction, leading to the considerable lowering of their orbital energies. The σ-type orbital is stabilized more than the π-type orbitals as the tilted agostic C−H_{ag} bond can overlap with the 6d−5f hybrid orbitals on U (Figure 6). The agostic interaction between C−H σ-bond and U empty orbitals can be viewed as formation of a three-centered two-electron bond. The UF_2 fragment has an electronic configuration of $(7s)^1(5f)^3$, where the 5f orbitals are transformed into $2a_1 + a_1 + 2b_1 + 2b_2$ in the C_{2v} symmetry. Upon coordination by the CH_2 fragment, two electrons are lost from U(II) and the 7s orbital is significantly pushed up in energy while the $5f^2$ band is destabilized. Interestingly, when the molecule is distorted into the agostic structures (C_1 symmetry) the $5f^2$ band is notably broadened, consistent with the enhanced bonding between U and the agostic C−H_{ag} bond. Indeed, the predicted U···H_{ag} distances (2.32−2.34Å) are much shorter than the sum of the van der Waals radii of U and H (3.06 Å), and the calculated Wiberg bond orders for U···H_{ag} are around 0.04−0.05 in these complexes, indicating a weak interaction between U and the H_{ag} atoms.

The Wiberg bond order of C═U decreases from 1.47 for CH_2═UCl_2 to 1.43 for CH_2═UF_2, indicating that the C═U bonds are slightly weakened with the more electronegative ligand attached to the U atom. This trend is consistent with the optimized C═U distances and the calculated diabatic bond energies listed in Table 4. The fact that the C═U double bonds are slightly weaker in the fluoride species than in the chloride species can be traced back to the radial contraction of the U 6d/5f orbitals by the inductive effect of the fluorine substituent. A similar effect was also found for the C≡U triple bonds in the HC≡UX_3 molecules.[47]

As expected, the calculated natural charges show that the agostic H atoms carry slightly less positive charge than the nonagostic H atoms. The U atoms carry highly positive charges, particularly, in the fluorides (Table 5). The analysis of the calculated natural localized molecular orbitals indicates that the halogen ligands are truly ionic in these complexes,

(47) Lyon, J. T.; Hu, H.-S.; Andrews, L.; Li, J. *Proc. Natl. Acad. Sci. U.S.A.* **2007**, *104*, 18919.

Table 6. Natural Occupation Number and NLMO Compositions for Methylidene Complexes from NBO Analysis

bond	occupation no. (α)	NLMO	occupation no. (β)	NLMO
		CH_2═UF_2		
U−Cσ	0.99	23% U($s^{0.30}p^{0.08}d^{0.97}f$) + 77% C($sp^{2.17}$)	0.99	19% U($s^{0.36}p^{0.11}d^{1.17}f$) + 81% C($sp^{1.94}$)
U−Cπ	0.99	36% U($d^{0.30}f$) + 64% C($s^{0.02}p^{1}$)	1.00	19% U($s^{0.03}d^{0.56}f$) + 81% C(p)
C−H_{ax}	0.99	60% C($sp^{1.49}$) + 40% H(s)	0.99	60% C($sp^{1.51}$) + 40% H(s)
C−H_{ag}	0.98	56% C($sp^{2.72}$) + 44% H(s)	0.98	56% C($sp^{2.83}$) + 44% H(s)
		CH_2═UFCl		
U−Cσ	0.99	23% U($s^{0.20}p^{0.05}d^{0.87}f$) + 77% C($sp^{2.33}$)	0.99	18% U($s^{0.32}p^{0.09}d^{1.18}f$) + 82% C($sp^{2.01}$)
U−Cπ	0.99	39% U($s^{0.06}d^{0.33}f$) + 61% C($s^{0.03}p$)	1.00	20% U($s^{0.06}p^{0.01}d^{0.85}f$) + 80% C($s^{0.01}p$)
C−H_{ax}	0.99	60% C($sp^{1.49}$) + 40% H(s)	0.99	61% C($sp^{1.51}$) + 39% H(s)
C−H_{ag}	0.97	56% C($sp^{2.72}$) + 44% H(s)	0.98	57% C($sp^{2.88}$) + 43% H(s)
		CH_2═UCl_2		
U−Cσ	0.99	26% U($s^{0.08}p^{0.02}d^{0.15}f$) + 74% C($sp^{3.80}$)	0.99	19% U($s^{0.26}p^{0.07}d^{1.11}f$) + 83% C($sp^{2.07}$)
U−Cπ	0.99	35% U($s^{0.13}p^{0.02}d^{0.52}f$) + 65% C($s^{0.14}p$)	1.00	21% U($s^{0.08}p^{0.02}d^{0.93}f$) + 79% C($s^{0.02}p$)
C−H_{ax}	0.99	60% C($sp^{1.49}$) + 40% H(s)	0.99	61% C($sp^{1.50}$) + 39% H(s)
C−H_{ag}	0.97	56% C($sp^{2.75}$) + 44% H(s)	0.97	57% C($sp^{2.95}$) + 43% H(s)

consistent with the U(IV) oxidation states. The U−F and U−Cl bond orders are much smaller than the C═U or C−H bonds. The C═U double bonds are highly polarized, with most electron density on C atoms, as shown by the NLMO compositions listed in Table 6. The calculated natural hybrid orbitals reveal that the U−C σ bond is mainly formed between the U 6d−5f hybrid orbital and C 2s−2p hybrid orbital, whereas the U−C π bond is formed between U 6d−5f hybrid orbital and nearly pure C 2p hybrid orbital. Of particular interest are the C hybrid orbitals involving the agostic H atoms. While nonagostic C−H bonds involve C sp hybrid orbitals, the agostic C−H bonds involve approximately a C sp^3 hybrid orbital, which is consistent with the longer C−H_{ag} distances and the U···H_{ag} agostic interaction. The fact that all these uranium methylidene complexes favor agostic structures rather than the symmetric structures is a natural result of the optimized orbital interaction in the agostic form, which has significant stabilization energy when comparing to a nonagostic strcuture.[22] These structural and bonding analyses have demonstrated differences between the uranium complexes and thorium or transition-metal analogues, thus underscoring the important role of f-orbitals in chemical bonding of heavy-element complexes.

Conclusions

Reactions of laser ablated U atoms with methylene halides form the actinide methylidene complexes CH_2═UXY (XY = F_2, FCl, Cl_2) as the major products. These molecules are identified through the matrix-isolation infrared spectra, isotopic frequencies, and comparison to frequencies and isotopic shifts calculated by using density functional theory. The popular hybrid B3LYP functional performs poorly for these methylidene complexes with C═U double bonds. The B3LYP structures for the CH_2═UXY complexes show larger ∠H−C−U angles, indicating less agostic distortion. The B3LYP spin contaminations of these complexes from higher spin states are rather large, leading to a longer C═U bond and erroneously low C−U stretching frequency, which is 117 cm^{-1} below the observed value for CH_2═UF_2. The pure PW91 density functional predicts structures with significant agostic distortion and the correct C═U stretching mode. The calculated vibrational frequencies and isotopic frequency shifts are in excellent agreement with those observed in the argon-matrix experiments. Detailed structural and bonding analyses show that these actinide methylidene complexes have significant bonding interactions between the U 6d/5f orbitals and the C 2s/2p orbitals, with the C═U bond strength tunable by attaching different substituents on uranium. The U 5f band is significantly broadened through the agostic interaction with hydrogen atoms. The low-lying 6d−5f orbitals form the foundation of the energetic preference of agostic structures for these actinide methylidene complexes.

Acknowledgment. We gratefully acknowledge the National Science Foundation and the NNSFC (20525104) and NKBRSF (2006CB932305, 2007CB815200) of China for financial support of this research. The calculations were performed by using a HP Itanium2 cluster at Tsinghua National Laboratory for Information Science and Technology.

IC701786H